Journal of Applied Polymer Science

Polypropylene/Silica Micro- and Nanocomposites Modified with Poly(styrene-*b*-ethylene-*co*-butylene-*b*-styrene)

Anđela Pustak,[1] Matjaž Denac,[2] Mirela Leskovac,[3] Iztok Švab,[4] Vojko Musil,[2] Ivan Šmit[1]

[1]Ruđer Bošković Institute, Division of Materials Chemistry, Bijenička 54, 10002 Zagreb, Croatia

[2]University of Maribor, Faculty of Economics and Business, Department of Techology and Entrepreneurial Enviroment Protection, Institute of Techology, Razlagova 14, 2000 Maribor, Slovenia

[3]University of Zagreb, Faculty of Chemical Engineering and Technology, Department of Surface Engineering of Polymer Materials, Savska 16, 10 000 Zagreb, Croatia

[4]ISOKON, Production and Processing of Thermoplastics, Ltd, Mestni trg 5a, 3210 Slovenske Konjice, Slovenia

Correspondence to: A. Pustak (E-mail: apustak@irb.hr) and M. Denac (E-mail: matjaz.denac@uni-mb.si)

ABSTRACT: The effects of different silica loadings and elastomeric content on interfacial properties, morphology and mechanical properties of polypropylene/silica 96/4 composites modified with 5, 10, 15, and 20 vol % of poly(styrene-*b*-ethylene-*co*-butylene-*b*-styrene) SEBS added to total composite volume were investigated. Four silica fillers differing in size (nano- *vs.* micro-) and in surface properties (untreated *vs.* treated) were chosen as fillers. Elastomer SEBS was added as impact modifier and compatibilizer at the same time. The morphology of ternary polymer composites revealed by light and scanning electron microscopies was compared with morphology predicted models based on interfacial properties. The results indicated that general morphology of composite systems was determined primarily by interfacial properties, whereas the spherulitic morphology of polypropylene matrix was a result of two competitive effects: nucleation effect of filler and solidification effect of elastomer. Tensile and impact strength properties were mainly influenced by combined competetive effects of stiff filler and tough SEBS elastomer. Spherulitic morphology of polypropylene matrix might affect some mechanical properties additionally. © 2014 Wiley Periodicals, Inc. J. Appl. Polym. Sci. **2014**, *132*, 41486.

KEYWORDS: compatibilization; composites; mechanical properties; morphology; structure-property relations

Received 30 April 2014; accepted 29 August 2014

DOI: 10.1002/app.41486

INTRODUCTION

A remarkable progress in polymer–matrix composites as advanced materials has been achieved through functionalization of filler surfaces as well as by introduction of nanofillers and compatibilizers.[1–5] Isotactic polypropylene (iPP) is one of the most widely used commodity plastomers for composites owing to its outstanding properties and versatile applications.[1] Most published works of binary iPP/silica composites comprehend two aims: the crystallization study of these composites and the improvement of the mechanical properties.[6–11] Tensile and impact strength increased with filler content and were mostly affected by the type and the content of silica nanoparticles.[6] The reinforcing and/or the toughening effects of the used nanoparticles on the polymer matrix were found to be effective at low filler loadings (usually in content range 0.5–6%) in comparison to conventional fillers.[6–10] A few authors reported enhanced volume of the filler/matrix interphase fraction by grafting of macromolecules onto silica nanoparticles leading to improved toughness and tensile strength.[7–9] Unlike other authors, Pustak et al. observed steady decrease of the impact strength values with addition of the silica fillers.[10] On the contrary, steady increase of Young's modulus with increased silica content indicates preferable reinforcing effect of stiffer silica particles.[7–11]

However, in order to improve the interfacial stress transfer and to balance the toughness and stiffness in polymer composites an appropriate compatibilizer and/or a rubber toughening agent should be added. Additional enchancement of tensile and impact strength was achieved by addition of maleated polypropylene (PP-*g*-MAH) as a compatibilizer for binary iPP/SiO_2 composites presented in papers by Bikiaris et al. and Bouaziz et al.[12,13] The hydroxyl groups on the surface of silica nanoparticles react with maleic anhydride groups of PP-*g*-MAH leading to higher adhesion between iPP matrix and silica particles and finer dispersion of individual SiO_2 nanoparticles with reduced agglomeration.[12,13]

While the compatibilization of binary and ternary iPP composites was widely explored,[12–22] there are few papers dealing with

introduction of complex compatibilizer and/or impact modifier into binary iPP/silica composites.[14–22] Chen et al. combined reactive compatibilization with toughening in hybrid composite system of polypropylene with silica and polyurethane (PU) (PP/PP-*g*-NH_2/SiO_2-*g*-PU/PU).[14] The impact strength and ductility of these hybrid composites have been improved by elastomeric polyurethane component and by compatibilization through —NH_2 groups (onto PP) and PP chains grafted onto silica particles.[14] In work of Uotila et al. uniform dispersion of silica particles and aggregates throughout both phases (iPP matrix and and elastomeric EPR) has been revealed.[15] While ethylene/butyl acrylate (E/BA) and ethylene/butyl acrylate/maleic anhydride (E/BA/MAH) compatibilizers dragged the filler particles towards the EPR phase, in composite with PP-*g*-MAH compatibilizer silica particles were dominantly dispersed through the iPP matrix.[15] Obviously, the selectivity of silica particles depends on compatibilizer type beside its compatibilization efficiency in blends. In simplified PP/EPDM blend systems (double role of EPDM—as compatibilizer and impact modifier could be supposed) final morphology and mechanical properties depended on surface character of silica particles and processing. Martin et al. observed that hydrophilic silica aggregates tend to migrate within the elastomeric EPDM phase, whereas hydrophobic particles were homogeneously dispersed within the EPDM phase and at the iPP/EPDM interface.[16] Bazgir et al. have shown that silica particles tended to remain encapsulated by EPDM rubber when mixed with EPDM before the adding of iPP.[17] Encapsulated silica particles changed the EPDM/iPP viscosity ratio, and hence EPDM droplets size and mechanical properties in dynamically crosslinked EPDM/iPP 60/40 blend filled by silica.[17] Liu et al. have observed better filler dispersion by addition of PP-*g*-MAH and reduction of large silica aggregates. Silica was located preferentialy in PP/PP-*g*-MAH phase and this separated morphology as well as elastomeric ethylene-octene copolymer (POE) lead to impact properties improvement and stiffness-toughness balance.[18]

Only few studies highlighted toughening of the iPP/SiO_2 composite by styrenic block copolymers (SBC) as elastomeric impact modifiers.[19–22] Wang et al. have concluded that the stiffness-toughness balance of the iPP/silica /SBR composites has been established due to strong synergistic effect between the filler and the elastomer.[19] Mae et al. have observed that the elastic modulus and the strain values of iPP/SiO_2 composites modified with poly(styrene-*b*-ethylene-*co*-butylene-*b*-styrene) (SEBS) have depended on the selectivity of SiO_2 nanoparticles, i.e. are they inside or outside of dispersed elastomeric SEBS particles.[20] The most recent investigations of the iPP/SiO_2/SEBS composites with PP-*g*-MAH added as compatibilizer by Panaitescu et al. confirmed relatively good compatibility of the iPP/SEBS interface resulting in improvement of mechanical and dielectrical properties.[21,22] The location of filler and interactions played again the crucial role in determing the properties of such composite systems. On the other side, El-Midany and Ibrahim compared the efficiency of poly(styrene-*b*-ethylene-*co*-butylene-*b*-styrene) (SEBS) and maleated SEBS (SEBS-*g*-MAH) as compatibilizers.[23] Long and Shanks reported the idea of adding maleated SEBS (SEBS-*g*-MAH) and maleated ethylene/propylene copolymers to polypropylene composites not only as a toughening agents but also as compatibilizers between filler particles and the polypropylene matrix.[24] The maleated elastomers with reactive MAH groups may encapsulate the filler particles resulting in improved impact properties.[25] Although SEBS elastomer was widely applied as a compatibilizer for polymer blend systems, its application as impact modifier and compatibilizer in polypropylene composites has been reported in only recently published papers of Panaitescu et al. and Stribeck et al.[21,22,26]

Elastomers with encapsulation ability have been added to composites as compatibilizing agents in small amount (up to 5%) like other compatibilizers.[21,26] Accordingly, El-Midany and Ibrahim introduced in polypropylene filled with 3% white microsilica sand as mineral filler 2.5% and 5% of SEBS and SEBS-*g*-MAH.[23] While the introduction of microsilica filler deteriorated ductility of the sample, added SEBS and SEBS-*g*-MAH elastomers increased tensile and impact strength of composites.

Summarized idea for studying simplified ternary polypropylene/silica/elastomer composite system with elastomeric poly(styrene-*b*-ethylene-*co*-butylene-*b*-styrene) block copolymer (SEBS) as an effective impact modifier and compatibilizer has been also presented in this article. Because SEBS grafted with maleic anhydride (SEBS-*g*-MAH) forms preferentially compartmentalized and inverse core-shell morphology morphology as reported in our previous investigation in the iPP/SiO_2/SEBS composites very distinctive morphologies could be expected in the case of block copolymer without reactive MAH group—SEBS elastomer.[27] Moreover, serious studies of morphology and mechanical properties of ternary polypropylene composites correlated with thorough study of adhesion properties of such composites were absent up to now. The relation between interfacial properties and composite morphology will be analyzed by models calculated from adhesion parameters. Additionally, the investigations of iPP/SiO_2/SEBS composites were mainly performed by using nanosilica filler[6–22] and only one mineral microsilica filler without comparison of nano vs. micro.[11–23] Thereby, the comparison of the effects of four silica fillers differing in size (nano- *vs.* micro-) and in their surface properties—new hydrophobic nanosilica (Aerosil R7200) vs. hydrophilic parent (Aerosil 200) and hydrophobic microsilica (Sipernat D17) *vs.* hydrophilic parent (Sipernat 120), e.g. non-polar vs. polar—have been carried out. Accordingly, the effects of different silica fillers as well as varied contents of SEBS elastomer (up to 20 vol %—sufficiently for simultaneous toughening and compatibilization) on composites and spherulitic morphology and mechanical properties of composites were discussed within the context of adhesion-morphology-mechanical property relationships.

EXPERIMENTAL

Materials

Isotactic polypropylene used as polymer matrix was supplied by Basell, Netherlands. Block copolymer SEBS poly(styrene-*b*-ethylene-*co*-buthylene-*b*-styrene) was used as compatibilizer and elastomeric impact modifier (supplied by KratonPolymers). Sillica was used as filler: two proprietary microsilica fillers

Table I. The Properties of Used Materials

Polymer	Commercial name	Density (g cm^{-3})	MFI (g 10^{-1} min^{-1})	M_n (g mol^{-1})	M_w/M_n
iPP	Moplen HP501L	0.90	6.0[a]	120.000[c]	5.4
SEBS	Kraton G-1652	0.91	0.5[b]	65.900[c]	1.07
Filler	**Commercial name**	**Tapped density (g dm^{-3})**	**Surface modification**	**Specific surface area (m^2 g^{-1})**	**Particle size, d_{50}**
S-120	Sipernat 120	185	none	125	12 nm
D-17	Sipernat D17	150	2% of chem. bounded carbon	100	12 nm
A-200	Aerosil 200	~50	None	200	14.5 μm
A-R7200	Aerosil R-7200	~230	Methacryl-silane	150	10 μm

[a] According to ISO 1133 (230°C/2.16 kg).
[b] According to ISO 1133 (200°C/5 kg).
[c] Measured with exclusion chromatography with PS standard.

(unmodified Sipernat 120 and surface modified Sipernat D17) and two proprietary nanosilica fillers (unmodified Aerosil 200 and surface modified Aerosil R7200). All silica fillers were kindly supplied by Evonic Industries (Degussa), Essen, Germany. The properties of used polymers and fillers are listed in Table I.

Sample Preparation

Ternary iPP/SiO_2/SEBS composites were prepared in an oil-heated Brabender kneading chamber. The iPP/SiO_2 volume ratio was kept constant at 96/4 and 5, 10, 15, and 20 vol % of SEBS elastomer was added to 100 volume parts of composite (added 20 vol % of SEBS corresponds to 16.7 vol % of SEBS in total mass). The volume ratio of iPP/SiO_2 96/4 was chosen on the basis of our previous investigation of binary iPP/SiO_2 composites because the composites with this content ratio have exhibited the best tensile strength and the largest spherulites.[10,28] Relatively wide content range 0–20 vol % of added SEBS elastomer was used in order to research its efficiency as compatibilizer (5 vol %) as well as impact modifier and compatibilizer at higher SEBS content. The components were put into an oil-heated Brabender kneading chamber preheated up to 200°C with a rotor speed of 50 min^{-1} and then kneaded for 7 min. After homogenization, the melt was rapidly transferred to a preheated laboratory press and compression molded into 1- and 4-mm-thick plates. The pressing temperature was 220°C, pressure 100 bar and the pressing time of 14 min for 1-mm and 11.5 min for 4-mm-thick plates.

Testing Methods

Contact Angle Measurement. Surface free energies of used polymers and fillers, as well as their corresponding dispersive and polar components, were determined by measuring contact angle. Contact angles of the iPP and silica fillers were measured on a contact angle goniometer DataPhysics OCA 20 Instrument at temperature 23°C. Sessile drops (2 μL) of test liquids: water (distilled twice $\lambda = 1.33$ μL cm^{-1}), formamide (p.a. 99.5%, Fluka) and diiodomethane (p.a. 99%, Aldrich), at 23°C were used for the advancing contact angle measurements. The standard deviation of these measurements was less than 2°. The surface tensions of the test liquids used for contact angle measurements are presented in Table II.

Surface free energies of the iPP, SEBS elastomer and silica fillers, (γ_{lv}) were calculated using harmonic mean equation according to Wu's model presented with eq. (1)[30]:

$$\gamma_l(1+\cos\theta) = \frac{4\gamma_s^d\gamma_l^d}{\gamma_s^d+\gamma_l^d} + \frac{4\gamma_s^p\gamma_l^p}{\gamma_s^p+\gamma_l^p} \quad (1)$$

where γ^p was the dispersive and γ^d the polar component of the surface free energy (surface tension), γ_l and γ_s were the surface tension of liquid and surface free energy of solid, respectively. This evaluation method was integrated in the software (SCA 20) and was automatically carried out by the computer.

Scanning Electron Microscopy (SEM). A SIRION 400 NC scanning electron microscope (SEM) was used to study the morphology of ternary composites. Samples were fractured in liquid nitrogen and covered with gold before being examined with a microscope at an acceleration voltage up to 10 kV at various magnifications. All SEM micrographs are secondary electron images.

Tensile Tests. Tensile properties (Young's modulus, tensile strength at break, elongation at break) were measured according to ISO 527 standard using Zwick 147670 Z100/SN5A apparatus at 23°C and strain rate of 2 mm min^{-1}. For each sample, five measurements were carried out and the average values were calculated within standard deviation about 5%.

Notched Impact Strength. Notched impact strength was measured by Zwick apparatus at 25°C according to Charpy test (DIN 53453). For each sample, 12 measurements were carried out and the average values were calculated within standard deviation of about 5% as well.

Table II. Surface Free Energy (γ_l), Dispersion (γ_l^d), and Polar Components (γ_l^p) of Test Liquids for Contact Angle Measurements[29]

Test liquids	γ_l (mJ m^{-2})	γ_l^d (mJ m^{-2})	γ_l^p (mJ m^{-2})
Water	72.8	21.8	51.0
Formamide	58.0	39.0	19.0
Diiodomethane	50.8	50.8	0.0

Table III. The Adhesion Parameters Between Different Components of iPP/Silica/SEBS Composites for Possible Adhesion Pairs: Polymer/Elastomer, Polymer/Filler or Elastomer/Filler

	Adhesion parameters (mJ m^{-2})			
	Interfacial free energy γ_{AB}			
Possible adhesion pairs	eq. (3)	eq. (4)	Work of adhesion W_{AB}*	Spreading coefficient S_{AB}*
iPP/SEBS	0.76	1.44	63.7	−1.9
iPP/S-120	24.69	33.82	82.7	17.1
SEBS/S-120	17.81	28.45	88.5	25.1
iPP/S-D17	9.77	16.39	30.3	−35.3
SEBS/S-D17	10.46	15.86	28.5	−34.9
iPP/A-200	24.97	34.31	84.5	18.9
SEBS/A-200	18.17	29.14	90.2	26.8
iPP/A-R7200	10.43	16.15	83.6	18.0
SEBS/A-R7200	6.86	12.44	86.0	22.6

A-matrix, B-elastomer or filler; eq. (3) Ovens-Wendt's geometric mean equation; eq. (4) Wu's harmonic mean equation;* calculated from eq. (3).

Optical Microscopy (OM). A Leica light microscope (Model DMLS) coupled with a digital camera was used for observation of thin crossed microtomed sections (taken from 1-mm-thick plates) under crossed polarizers (POM) or phase contrast (PC). Maximal anisotropic diameter of spherulites ($d_{i,\max}$) was measured on several polarization micrographs of each sample and average spherulite diameter (d_{sph}) was calculated according to eq. (2):

$$d_{sph} = \frac{\sum N_i d_{imax}}{\sum N_i} \quad (2)$$

where N_i is the number of measured spherulites with the average diameter d_i.

RESULTS AND DISCUSSION

Interfacial Properties of the iPP/SiO_2/SEBS Composites

Domain morphology of ternary polymer blends and composites could be classified into three classes: separated, core-shell, and stacked morphology.[31] Because rare stacked domain morphology could be observed mainly in polymer composites containing anisotropic filler microparticles, the most probable morphology in presented composites with spherical silica particles would be according to the literature: separated (SM) and core-shell morphology (CS).[32] The appearance of the inverse core-shell (iCS) and compartmentalized core-shell morphology (cCS) could be also supposed; the last is known under different terms: morel structure, honeycomb-like morphology, and multiple inclusion or salami-like morphology.[33] Inverse core-shell morphology contains the continual interlayer of agglomerated particles that encapsulates dispersed elastomer particles in polymer matrix in distinct to discontinuous interlayer of nanoparticles or agglomerates at the interface.[16] The limits of ideal morphologies of the iPP/SiO_2/SEBS composites might be predicted by analysis of adhesion parameters (interfacial free energy, work of adhesion, spreading coefficient).

Adhesion Parameters of the iPP/silica/SEBS Composites

The values of surface free energies, γ of solids (with respectively dispersive, γ^d and polar component, γ^p values) were determined by measuring contact angles.[30] The calculated interfacial free energy, γ_{mf}, work of adhesion, W_{mf}, and spreading coefficient, S_{mf}, of all possible polymer/elastomer, polymer/filler and elastomer/filler pairs were calculated from obtained γ values using eqs. (2–5) and presented in Table III.

$$\gamma_{AB} = \gamma_A + \gamma_B - 2\sqrt{\gamma_A^d \gamma_B^d} - 2\sqrt{\gamma_A^p \gamma_B^p} \quad (3)$$

$$\gamma_{AB} = \gamma_A + \gamma_B - \frac{4\gamma_A^d \gamma_B^d}{\gamma_A^d + \gamma_B^d} + \frac{4\gamma_A^p \gamma_B^p}{\gamma_A^p + \gamma_B^p} \quad (4)$$

$$W_{AB} = \gamma_A + \gamma_B - \gamma_{AB} \quad (5)$$

$$S_{AB} = \gamma_B - \gamma_A - \gamma_{AB} \quad (6)$$

where subscripts A and B mean phases in composites (A-matrix, B- filler, elastomer) and superscripts d and p mean dispersed and polar components.

According to Steinman et al. interfacial free energy value calculated by Wu's harmonic mean eq. (4) should be taken into account for the analysis of polymer iPP-SEBS pair, whereas for high-energy polymer-filler pair interfacial free energy value calculated by Ovens-Wendt's geometric mean eq. (3) should be considered.[34] Effective adhesion between component pairs can be indicated by followed conditions as optimal: thermodynamic work of adhesion as maximal, spreading coefficient as a positive value and interfacial free energy or interfacial tension as a minimal.[30,34,35] According to these conditions all silica fillers, except S-D17 microsilica, selectively filled SEBS elastomer rather than iPP matrix. This result indicate the distribution of the S-120, A-200 and A-R7200 fillers preferentially in the SEBS phase by forming preferential core-shell and compartmentalized morphologies (CS and cCS). Small differences in the values of all three parameters between iPP-filler and SEBS-filler pairs lead to some inconsistencies. Because the adhesion work and the spreading coefficient values sometimes lead to incoherent conclusions, the interfacial free energy values seem to be more relevant for ambiguous systems.[36,37] Accordingly, some

Table IV. According to Model 1 Filler Migrates to the A–B Interface when Conditions are Fulfilled (Yes)

Ternary polymer composites	$\gamma_{AB}/2$	γ_{AF}	γ_{BF}	$\gamma_{AF}-\gamma_{AB}/2$	$\gamma_{BF}-\gamma_{AB}/2$	$\gamma_{AF} \geq \gamma_{BF}-\gamma_{AB}/2$	$\gamma_{BF} \geq \gamma_{AF}-\gamma_{AB}/2$
iPP/S-120/SEBS	0.72	24.69	17.81	17.09	23.97	Yes	No
iPP/S-D17/SEBS	0.72	9.77	10.46	9.74	9.05	Yes	Yes
iPP/A-200/SEBS	0.72	24.97	18.17	24.25	17.45	Yes	No
iPP/A-R7200/SEBS	0.72	10.43	6.86	9.71	6.13	Yes	No

A-matrix, B-elastomer, F-filler, γ_{AB} according to Wu's eq. (4), γ_{AF}, γ_{BF} according to Owens–Wendt's eq. (3).

lower interfacial free energy, γ_{AB}, for the iPP/S-D17 (9.77) pair than for SEBS/S-D17 pair (10.46) indicates preferable filler dispersion in the iPP matrix, i.e. preferential separated morphology (SM) in this composite. Because the selectivity of fillers for both phases (iPP and SEBS) concluded on the basis of γ values, decrease simultaneously in approximately the same order: S-D17 $\geq$ A-R7200 > S-120 > A-200, the difference $\Delta\gamma = \gamma_{iPP} - \gamma_{SEBS}$ could be additional indication for selectivity. The decrease of $\Delta\gamma$ values in order S-120 (6.88 mJ m^{-2}) > A-200 (6.80 mJ m^{-2}) > A-R7200 (3.50 mJ m^{-2}) > S-D17 (-0.69 mJ m^{-2}) may also indicate the decrease of selectivity for SEBS phase and increased selectivity for the iPP phase in this order. The S-D17 microsilica filler selectively filled the iPP matrix forming thus separated morphology (SM). Intermediary $\Delta\gamma$ value for composite with nanosilica A-R7200 may indicate some trend of partial forming of inverse core-shell morphology (iCS). Obviously, there is the change-over from preferable inverse core-shell morphology in the case of iPP/S-D17/SEBS-*g*-MAH composites to separated morphology (SM) in the iPP/S-D17/SEBS composites.[27]

Interfacial Free Energy Model 1. According to Clarke et al. the filler (F) will be located at the interface of two polymers (A and B) if two conditions are satisfied[38]:

1. migration of fillers from phase A to the interface:

$$\gamma_{AF} > \gamma_{BF} - \gamma_{AB}/2 \quad (7)$$

2. migration of fillers from phase B to the interface:

$$\gamma_{BF} > \gamma_{AF} - \gamma_{AB}/2 \quad (8)$$

where γ_{AF} and γ_{BF} are the specific excess interfacial free energies of the filler F in components A and B, respectively, while γ_{AB} is the specific excess interfacial free energy of the polymers.

According to the results in Table IV obtained by calculating with eqs. (7) and (8) unmodified S-120, A-200 silica fillers and modified A-R7200 nanosilica with polar surfaces distribute selectively in elastomer compartmentalized (salami) and encapsulated core-shell morphologies (CS, cCS). Only modified silica filler S-D17 tends to migrate from SEBS elastomer to the iPP matrix. Actually, the differences between left and right terms in eqs. (7) and (8) for the composite with S-D17 is close to positive zero what may indicate partial formation of inverse core-shell morphology (iCS).

Interfacial Free Energy Model 2. According to qualitative approach provided by Sumita et al. wetting coefficient, ω_a, which allows predicting selectivity of the filler, is calculated by eq. (9)[39]:

$$\omega_a = \frac{\gamma_{filler-B} - \gamma_{filler-A}}{\gamma_{A-B}} \quad (9)$$

where $\gamma_{filler-A}$ and $\gamma_{filler-B}$ are the interfacial tensions between the filler and polymer A or B and γ_{A-B} is the interfacial tension between polymers A and B.

According to this model:

$\omega_a > 1$ the filler distributes within the A-phase; $-1 < \omega_a < 1$ filler is located at the interface and

$\omega_a <$ -1 the filler distributes within phase B.

According to the results in Table V silica fillers S-120, A-200 and A-R7200 remain in elastomeric SEBS phase enabling preferential forming of the core-shell morphology varieties (CS, cCS). Because modified microsilica S-D17 fulfilled $-1 < \omega_a < 1$ condition ($\omega_a = 0.48$), the filler should be alocated prefentially in the interphase forming the inverse core-shell morphology (iCS). However, this ω_a value is very close to fulfill of $\omega_a > 1$ condition and might at least imply partly distribution of S-D17 filler within the A-phase (iPP).

Spreading Coefficient Concept (Model 3). Hobbs et al. used Harkins spreading coefficient concept for interpreting or predicting the morphology of different ternary blends.[40] For a ternary system with A as the matrix phase and with B and F as the dispersed phases, the spreading coefficient λ_{AF} of the A-phase on the F-phase is simply according to eq. (10):

Table V. Filler Location Calculated According to the Model 2

Ternary polymer composites	γ_{AB}	$\gamma_{filler-A}$	$\gamma_{filer-B}$	ω_A	Filler location
iPP/S-120/SEBS	1.44	24.69	17.81	−4.77	Phase B
iPP/S-D17/SEBS	1.44	9.77	10.46	0.48	Interphase
iPP/A-200/SEBS	1.44	24.97	18.17	−4.71	Phase B
iPP/A-R7200/SEBS	1.44	10.43	6.86	−2.48	Phase B

A-matrix, B-elastomer, F-filler; γ_{AB} according to Wu's eq. (4), γ_{AF}, γ_{BF} according to Owens–Wendt's eq (3).

Table VI. Harkins Spreading Coefficients of iPP/Silica/SEBS Polymer Composites

Ternary polymer blends	γ_{AB}	$\gamma_{filler\text{-}A}$	$\gamma_{filer\text{-}B}$	$\lambda_{A\text{-}F}$	$\lambda_{A\text{-}F}^{*}$
iPP/S-120/SEBS	1.44	24.69	17.81	−8.32	5.44
iPP/S-D17/SEBS	1.44	9.77	10.46	0.76	−2.13
iPP/A-200/SEBS	1.44	24.97	18.17	−8.24	5.32
iPP/A-R7200/SEBS	1.44	10.43	6.86	−5.02	2.13

A-matrix, B-elastomer, F-filler;*A-elastomer, B-matrix, F-filler; γ_{AB} according to Wu's eq. (4), γ_{AF}, γ_{BF} according to Owens–Wendt's eq. (3)

$$\lambda_{AF}=\gamma_{BF}-\gamma_{AB}-\gamma_{AF} \quad (10)$$

where γ_{BF} is the interfacial tension between the phase B and the filler, γ_{AB} is the interfacial tension between the phase A and B, and the γ_{AF} is the interfacial tension between the phase B and the filler. If λ_{AF} is positive, the A-phase will encapsulate the F-phase while $\lambda_{AF}<0$ indicates separated phases A and F. The λ_{AF} tends to nul if the F (filler) migrates to interphase between the A and B phases.

Higher positive Harkins' spreading coefficient values, λ_{AF} mean stronger interactions between dispersed filler particles and polymer. Accordingly, positive $\lambda_{A\text{-}F}^{*}$ values for composites with untreated polar fillers S-120 (micro) and A-200 (nano) (Table VI) indicate good interactions between these silica particles and SEBS phase indicating preferential formation of core-shell morphologies (CS and cCS).

Because λ_{AF} values of the iPP/S-D17/SEBS composite tend to nul the tendency of interphase location of the S-D17 fillers could be supposed (inverse core-shell morphology, iCS). Somewhat negative $\lambda_{A\text{-}F}^{*}$ may indicate possible migration of this filler from SEBS phase and its spreading into iPP matrix.

Predicted Morphologies of the iPP/SiO_2/SEBS Composites. According to the analysis of the results in Tables III–VI the most probable morphologies in these composites could be supposed. Predicted morphologies in presented iPP/SiO_2/SEBS composites are rather a spectrum of all possible morphologies: CS, cCS, iCS, and SM (Table VII). These results are in accordance to findings in literature that the filler is not fully located in one phase but migrates to a certain extent into the second polymer and/or into the interface.[34] However, the results in Table VII indicated one or eventual two dominant morphology types in every composite. Accordingly, in the composites with Hydrophilic silica fillers the most probable morphologies would be compartmentalized (salami) or core-shell (cCS, CS). Composites with hydrophobic S-D17 microsilica would exhibit preferentially separated (SM) or inverse core-shell morphology (iCS). Composites with A-R7200 nanosilica with intermediary criterium values would exhibit rather spectrum of morphologies (CS, cCS, iCS, and SM).

Morphology of the iPP/SiO_2/SEBS Composites

Scanning Electron Microscopy (SEM). Bright spots on SEM micrographs in Figure 1(a,b) are related with micron- and nano- sized silica particles and their aggregates. Dark hollows in these SEM micrographs originate from dispersed SEBS particles and seldom from holes from which filler particles were pulled-out. Micron-sized S-120 and S-D17 silica particles with sizes $d_{SiO2}>3$ μm (corresponding to maximal d_{SEBS}) were mainly pulled out from the fractured composite surfaces. Smaller micron-sized particles (up to ~3 μm) were mainly remained within SEBS holes at fractured surfaces forming core-shell morphology (CS) [Figure 1(a,b)]. The aggregates of tiny S-120 particles (smaller than 1 μm) completely fulfilled dark SEBS holes in the case of iPP/S-120/SEBS composite with added 10 vol % of SEBS forming thus preferentially complex compartmentalized (multiple inclusion) morphology (cCS) (not shown). This sample with 20 vol % of SEBS exhibits also some dark hollows [Figure 1(a)] resembling to inverse core-shell morphology (iCS) due to enlarged dispersed SEBS particles. Ternary iPP composite with 20 vol % of modified nonpolar S-D17 microsilica reveals dark hollows engulfing micron-sized S-D17 particles or compact aggregates [Figure 1(b)]. Tiny S-D17 particles and their aggregates are preferentially dispersed in the iPP matrix [Figure 1(b)] and partly form irregular inverse core-shell (iCS) morphology [inserted picture in Figure 1(b) with higher magnification]. Observed preferable cCS and CS morphologies in the case of S-120 filler and separated morphology (SM) in the case of S-D17 filler are the best described by model 2 (Sumita et al.) but they are also in accord to morphologies predicted by model 3 (Hobs

Table VII. Predicted Morphologies on the Basis of Proposed Concepts

	Possible morphologies of ternary composites iPP/silica/SEBS			
Calculation model	iPP/S-120/SEBS	iPP/S-D17/SEBS	iPP/A-200/ SEBS	iPP/A-R7200/ SEBS
AP of CP[a]	CS + cCS	SM	CS+cCS	CS+cCS
Model 1	CS+cCS	iCS	CS+cCS	CS+cCS+iCS
Model 2	CS+cCS	SM + iCS	CS+cCS	CS+cCS+iCS
Model 3	CS+cCS	iCS+SM	CS+cCS	CS+cCS+iCS

[a] Adhesion parameters of the component pairs.

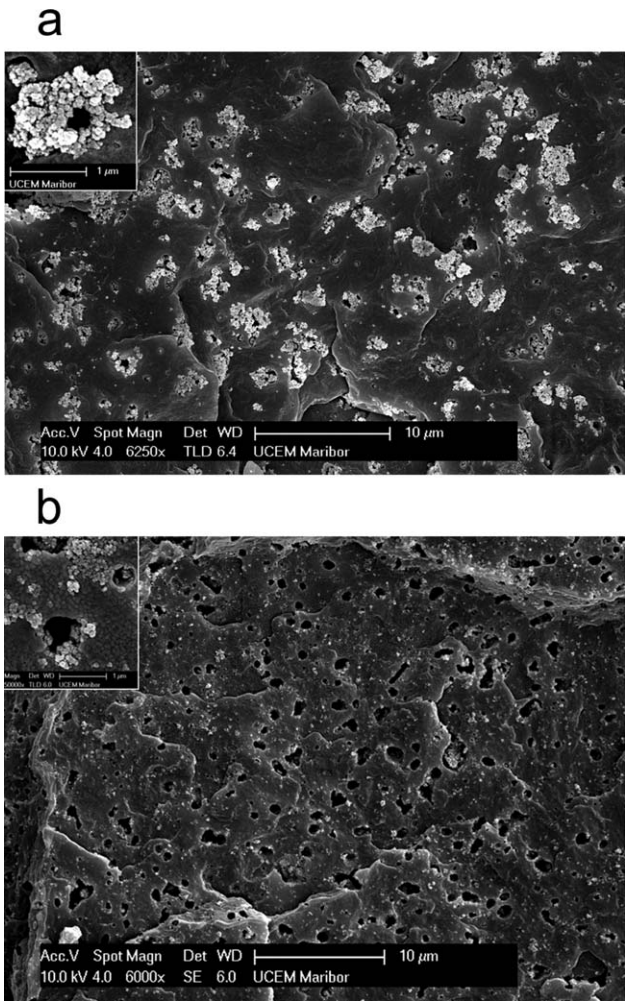

Figure 1. SEM micrographs of (a) the iPP/S-120 96/4 composite and (b) iPP/S-D17 96/4 composite modified with 20 vol % SEBS.

et al.) and by adhesion parameters of the component pairs—first row in Table VII.[39,40]

Ternary iPP composites with polar A-200 nanosilica [Figure 2(a)] exhibit the morphology alike agglomerated submicron-sized particles in the iPP/S-120 composites. Prevalent morphology in this composite is complex compartmentalized morphology (cCS). Some part with iCS morphology could be result of enlarged dispersed SEBS particles rather than common trend of this filler. Composites with methacrylsilanized A-R7200 nanofiller exhibit wider spectrum of morphologies with two specificity of these morphologies: huge nanosilica agglomerates and very irregular and complex morphologies [Figure 2(b)]. Complex compartmentalized morphology (cCS) of composites with polar A-200 nanosilica was predicted by all models as well as by adhesion parameters of the component pairs (Table VII).

Models 1–3 also predicted wide spectrum of morphologies CS+cCS+iCS for composites with methacrylsilanized A-R7200 nanofiller (Table VII) except separated morphology (SM) observed in Figure 2(b). However, some tendency for selectivity of A-R7200 nanoparticles in the iPP matrix might be assumed from models values between composites with S-D17 and composites with S-120 and A-200 fillers (see ω_a values in Table V for model 2).

In general, it seems that the composite morphologies are determined primarily by interfacial properties between components. Similar morphologies between composites with untreated, hydrophilic silica particles (micro S-120, nano A-200) illustratively confirm stronger influence of particle adhesion than the particle size. Additional influence of polymer viscosity ratio to the morphology could be supposed with increased elastomer content in the case of fillers with hydrophilic surface (S-120, A-200). Actually, SEM micrographs of presented composites reveal the spectrum of morphologies (CS, cCS, iCS, and SM) with one or just two preferential morphologies in every sample (Figures 1 and 2). Presented results confirm common findings in literature that the filler is not fully located only in one phase or only at interface.[34]

Spherulitic Morphology of the iPP/SiO_2/SEBS Composites. Polarization micrographs of binary iPP/silica composites indicated that silica particles with polar surfaces like A-R7200 more significantly decreased the spherulite size than silica particles with hydrophobic, non-polar surfaces like S-D17 due to stronger nucleation effect.[24] Introduction of even 4 vol % of A-R7200 decreases spherulites to scarcely cognizable forms [Figure 3(b)].

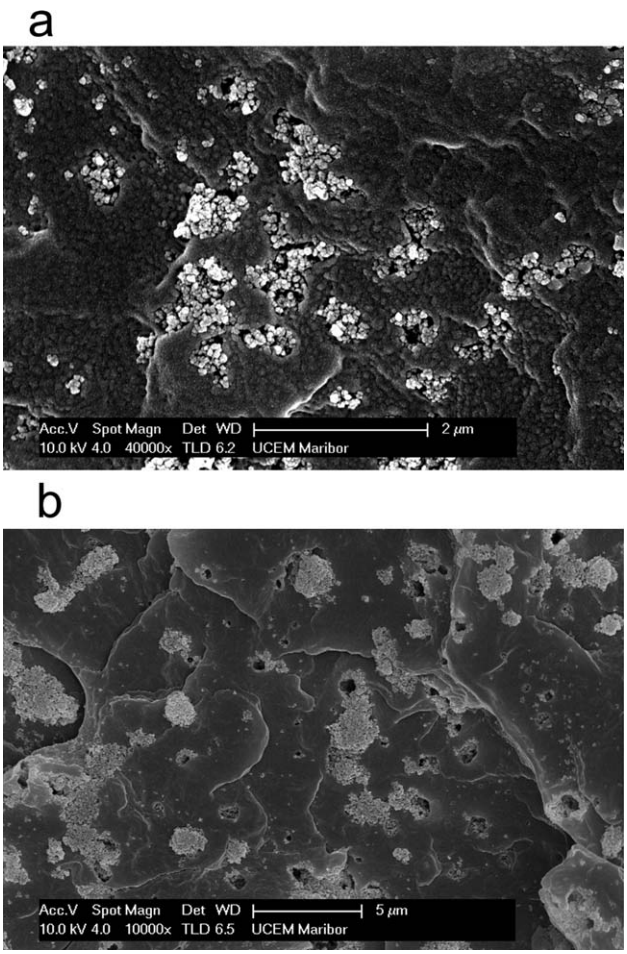

Figure 2. SEM micrographs of (a) the iPP/A-200 96/4 and (b) the iPP/A-R7200 96/4 composite with 20 vol % of added SEBS.

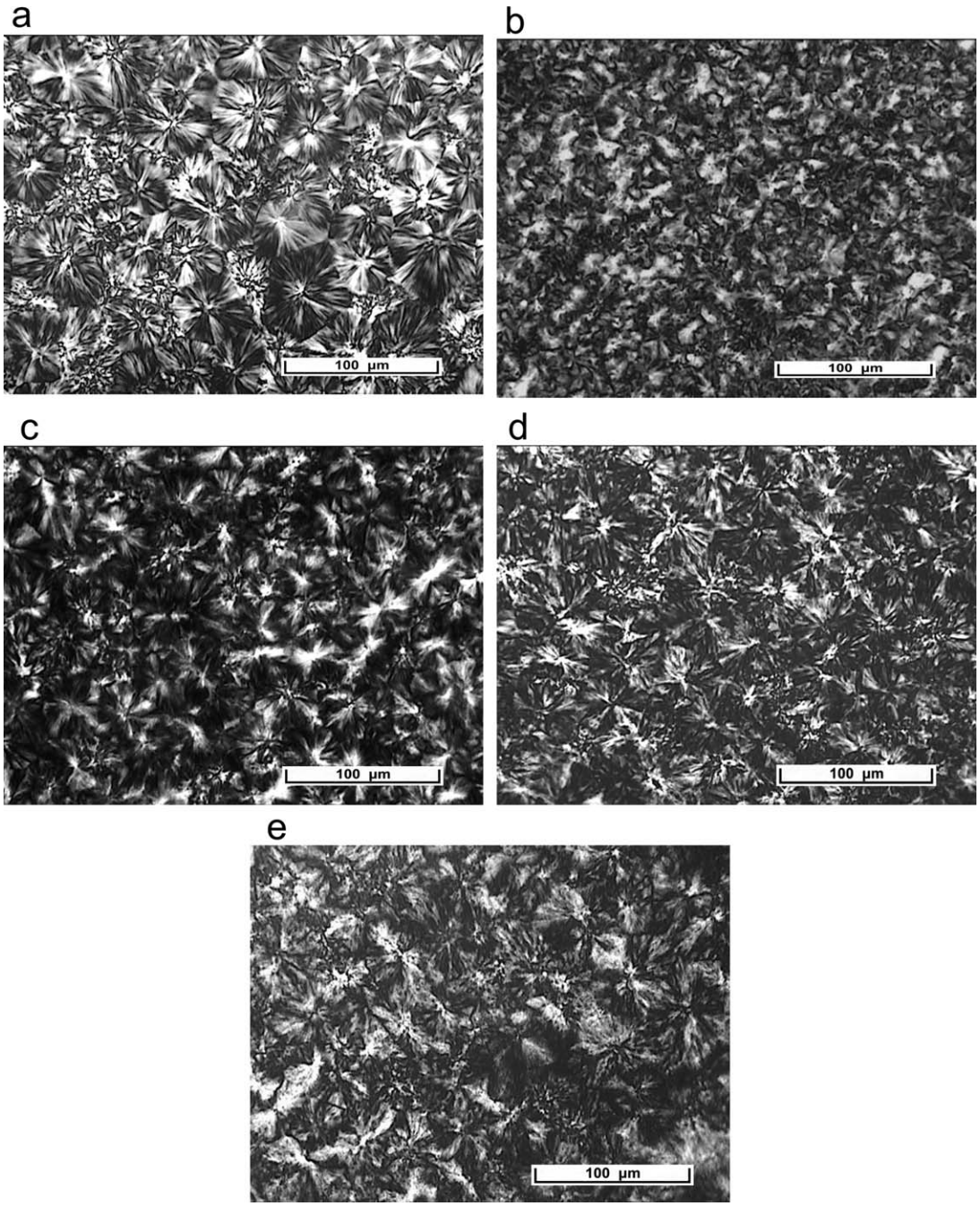

Figure 3. Polarized optical micrographs of (a) neat iPP, (b) binary iPP/A-R7200 96/4 composite, (c) iPP/A-R7200 96/4 composite with 10 vol % of SEBS, (d) iPP/A-R7200 96/4 composite with 20 vol % of SEBS, and (e) iPP/S-D17 96/4 composite with 20 vol % of SEBS.

The addition of the SEBS elastomer into iPP/silica composites increases the spherulite size in all composite systems (illustrated with polarization micrograps of the iPP/A-R7200 composites with added 10 and 20 vol % of SEBS in Figure 3(c,d)] what indicates overcoming influence of the solidification. Migration of iPP chains from the remaining melt islands of the SEBS elastomer toward the iPP matrix and their crystallization during solidification of molten composite was prolonged. Moreover, nucleation ability of polar A-R7200 nanoparticles in ternary composite could be reduced in comparison to binary composite due to partial encapsulation of particles by dispersed SEBS elastomer particles [Figure 2(b)]. This fact might enhance spherulite growth additionally. On the other side, silica S-D17 particles with the weakest nucleation ability due to compatible iPP−S-D17 interface may contribute to the largest spherulites [see Figure 3(e)] despite of preferentially separated S-D17 particles in the iPP matrix.[24,41]

Schematic presentation (intermediar picture) constructed on the basis of optical (left) and polarizing (right) micrographs of the iPP/S-D17 96/4 composite with 20 vol % of SEBS (Figure 4)

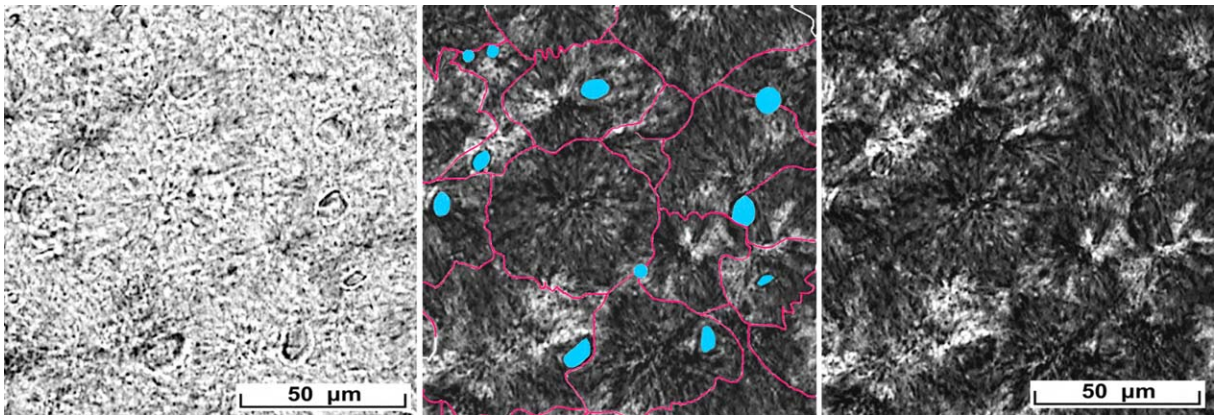

Figure 4. Light micrographs of the iPP/S-D17 96/4 composite modified with 20 vol % of SEBS taken under parallel (left) and crossed polars (right) as well as their schematic presentation (intermediary). [Color figure can be viewed in the online issue, which is available at wileyonlinelibrary.com.]

exhibits the relation between dispersed SEBS particles, micron-sized filler particles and iPP spherulites. Dispersed elastomeric SEBS particles with relatively narrow particle size distribution (dark spots of dispersed particles with sizes up to 3 μm in SEM micrographs visible in OM micrographs in Figure 4) are accommodated intraspherulitically and interspherulitically.[27,42] Preferentially radial intraspherulitical alignment of dispersed SEBS particles and nanosilica aggregates between growing bundles of lamellae might be supposed during the crystallization as proved in ternary iPP/silica/SEBS-g-MAH and in binary iPP/silica composite.[10,27,28] Schematic presentation in Figure 4 reveals mainly interspherulitic acommodation of large micro-sized S-D17 particles beside some S-D17 particles engulfed by iPP spherulites. This fact could not explain are these microparticles ejected to the spherulite surfaces or they stopped the spherulite growth regardless of their nucleation ability.

Generally, silica filler and SEBS elastomer affect the spherulite growth in the iPP matrix by two opposite, competitive effects: nucleation effect of filler and solidification effect of elastomer [Figure 3(a–e)]. It seems that the morphologies of composites observed by SEM may somewhat affect nucleation what contributes to the spherulitic morphology in lesser extent.

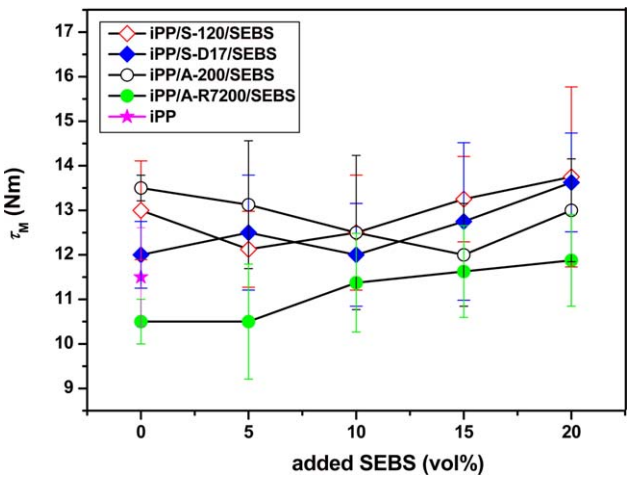

Figure 5. Steady state torque moment of the iPP composites in dependance on SEBS volume content. [Color figure can be viewed in the online issue, which is available at wileyonlinelibrary.com.]

Steady State Torque Moment of the iPP Composites. The torque moment value (τ_M), as a measure of melt viscosity, gives the information how SEBS modifier and silica filler affect processabillity of the iPP/silica/SEBS composites. Torque moment increases by adding every component in batch mixer, decreases after the polypropylene melting and reaches constant value around 6th minute of the mixing (measured τ_M values in Figure 5) due to homogenization and equalized viscosity of composites.[43] The τ_M values of the iPP composites change slightly or even negligible with addition of SEBS elastomer. The behavior of molten composites with S-120, A-200 and S-D17 fillers is similar and their τ_M values are higher than value for composite with modified A-R7200 nanosilica. Obviously, uncoated/untreated silica fillers with hydrophilic surfaces (S-120 and A-200) as well as microsilicas (S-10 and S-D17) contribute to higher melt viscosity than coated/treated nanofillers (A-R7200). Higher torque τ_M values of silica particles with hydrophilic surfaces can be ascribed to —OH groups. Moreover, higher viscosities of molten composites with micro-sized filler particles than with nano-sized filler are in an according to findings of Das et al.[44]

Tensile Test

Young's Modulus. While Young's modulus steadily rises with increased filler content due to reinforcing effect of filler,[28,45] the addition of SEBS elastomer to the iPP/silica composite reduces composite stiffness as was shown by Figure 6. Young's modulus of all ternary iPP/silica/SEBS composites decreases steadily upon the addition of SEBS elastomer. Almost liner decrease of the E values is combined stiffening filler and toughening elastomer effects rather than the result of some morphological or microstructural changes.[15,18,46] Such resulting decrease of the E values in ternary composites obviously is caused by prevailing toughening effect of the SEBS elastomer.

Tensile Strength and Elongation at Break. The incorporation of various filler and elastomer modifiers into polymers often have complex influence to the tensile strength at break, σ_b: increasing, decreasing or without any visible effect on tensile

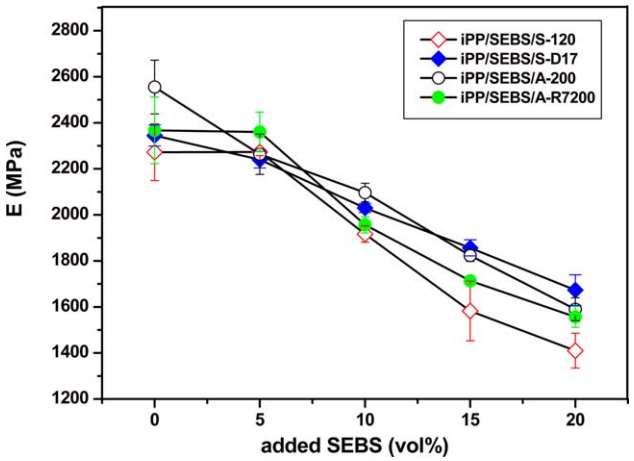

Figure 6. Young's modulus of ternary iPP/SiO_2/SEBS composites in dependence on elastomer content. [Color figure can be viewed in the online issue, which is available at wileyonlinelibrary.com.]

strength.[2,3] Actually, the addition of SEBS modifier to the iPP/silica composites decreases σ_b values [Figure 7(a)] monotonously. Altough σ_b values of the composites with modified filler S-D17 exhibit high standard deviation they are somewhat lower than those ones with three other fillers (S-120, A-200, A-R7200). On the other side, elongation at break, ε_b, usually behaves inversely to the tensile strength at break [Figure 7(b)]. Considering the highest compatibility between iPP and S-D17 particles the highest tensile strength in these composites could be expected. However, iPP-silica interface is only one influencing factor. The result could be reasonable if we take consider the largest spherulites in the composites with S-D17 silica–filler particles with the weakest nucleation ability due to compatible iPP−S-D17 interface [see Figure 3(e)]. More expressive differences (maximal spherulite size and minimal σ_b values for composites with S-D17 in respect to other three composites) observed in binary iPP/SiO_2 system have confirmed the influence of spherulite size.[10,24] Moreover, this ternary composites exhibit preferentially separated morphology in respect to other three systems. It could be supposed that the tensile strength of separated morphology is inferior in comparison to ones with core-shell or compartmentalized morphology.

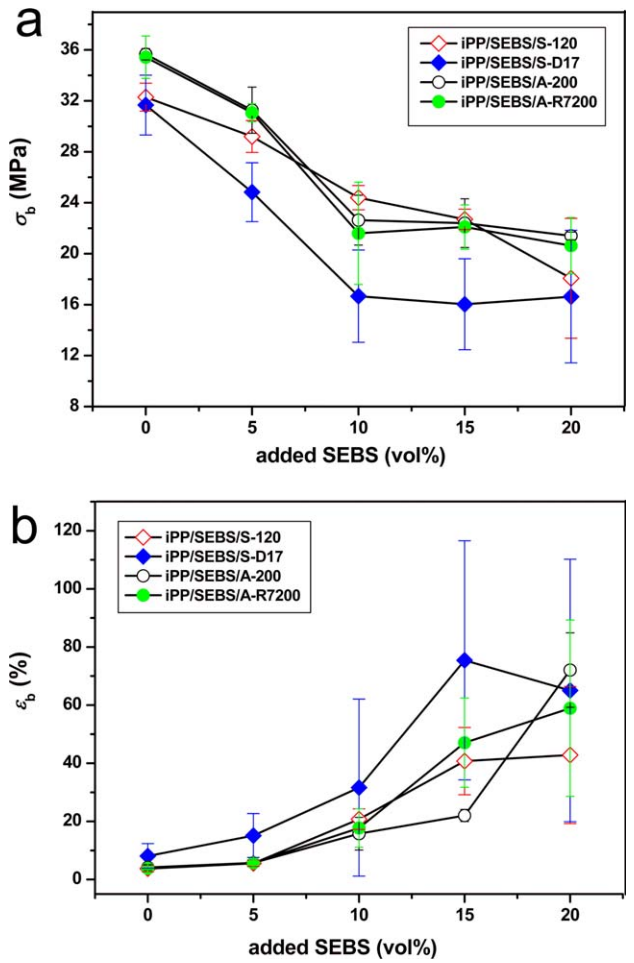

Figure 7. (a) Tensile strength and (b) elongation at break of the iPP/SiO_2/SEBS composites in dependence on elastomer content. [Color figure can be viewed in the online issue, which is available at wileyonlinelibrary.com.]

Impact Properties. The incorporation of silica filler usually improves stiffness and tensile strength but sometimes reduces the toughness leading to poorer impact strength as was refered in our previous work.[28] The balance of the mechanical behavior of such polymer-matrix composite materials might be achieved by addition of proper impact modifier. Thereby, SEBS elastomer was added to the binary iPP/SiO_2 composites in order to increase its toughness. Really, notched impact strength of the iPP/silica composites decreases with increased silica content.[28] On the contrary, impact strength, a_K, of the iPP/SiO_2/SEBS composites steady increases by the addition of SEBS elastomer (Figure 8). Thereby, the composites containing 20 vol % of loaded elastomer exhibit approximately fourfold increase of the a_K values in respect to binary composites. This fact indicate significant overcome of elastomeric toughening effect regarding to stiffening effect of the filler leading to the decrease of impact strength.[10] Impact strength values of all composites are very close and they are rather the consequence of synergistic effect of introduced SiO_2 and SEBS (stiffening by filler and toughening

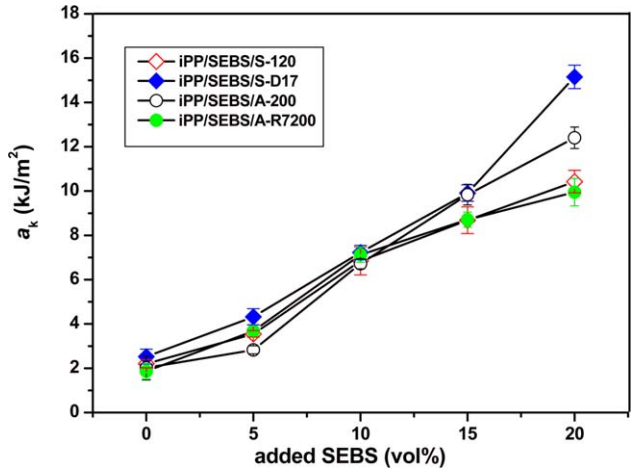

Figure 8. Notched impact strength of the iPP/SiO_2/SEBS composites in dependence on elastomer content. [Color figure can be viewed in the online issue, which is available at wileyonlinelibrary.com.]

by elastomer) analogously to effect observed in iPP/SiO_2/SBR composites by Wang et al.[19] Spherulitic morphology of ternary composites may affects impact strength additionally (see composite with S-D17 at 20 vol % of added SEBS) leading to more scaterred values which exceed standard deviation values (Figure 8). Therefore, this scaterred values at 20 vol % of added SEBS may arise from physical reasons. It is possible that increased toughening at higher SEBS elastomer content was superponed by differently developped spherulites. For example, S-D17 microparticles dispersed manly in the iPP matrix exhibit weaker nucleation ability in respect to other fillers due to better compatibility with iPP matrix. This fact leads to larger spherulites in binary iPP/S-D17 composite[24] and in presented ternary iPP/S-D17/SEBS composite [see Figure 3(e)] in respect to other composites. Thereby, spherulite size seemed to be more probable additional influential factor than interfacial strength between components.

CONCLUSIONS

Morphology of particular iPP/SiO_2/SEBS composite was determined primarily by interfacial properties. There are proven common literature findings that real morphology of every composite is a spectrum of several morphologies rather than one exclusive morphology. Studied iPP/SiO_2/SEBS composites with untreated hydrophilic fillers revealed preferentially compartmentalized morphology (salami or morphology with multiple inclusion). Composites with hydrophobic S-D17 microsilica exhibited preferentially separated (SM) morphology in comparison to preferable inverse core-shell morphology (iCS) in iPP/S-D17/SEBS-*g*-MAH composites. Composites with modified A-R7200 nanosilica exhibit rather spectrum of morphologies (CS, cCS, iCS, and SM).

Dispersed elastomeric SEBS particles are accommodated intra- and interspherulitically. Intraspherulitically aligned SEBS and nanosilica particles seems to follow radial accommodation into radial growing of lamellae during the crystallization. Tensile and impact strength properties were influenced by combining effects of stiff filler and toughened SEBS elastomer rather or more significantly than by other factors. Some tensile and impact strength properties might be affected by spherulitic morphology of ternary iPP/SiO_2/SEBS comoposites additionally.

GROUP AUTHORSHIP INFORMATION

Substantial contribution and acquisition of all data given in this article, interpretation and critical analysis of this data as a part of collaboration work between investigation groups must be given to Dr. Anđela Pustak and Dr. Matjaž Denac equally. Big part of obtained and interpreted data are a part of PhD thesis of A. Pustak. For revising the article and giving the critical opinion and also by helping to design this article, the credits must be given to Dr. Ivan Šmit. Dr. Vojko Musil contributed as a senior researcher giving the critical point note to observed and interpreted data especially for mechanical properties. Dr. Mirela Leskovac helped us to obtain and to interpretate valuable data for calculating surface free energy and adhesion parameters. Dr. Iztok Švab gave valuable contribution to measuring some interfacial and mechanical properties.

ACKNOWLEDGMENTS

Financial support of the Ministry of Science, Education and Sports of the Republic of Croatia and the Ministry of Higher Education, Science and Technology of the Republic of Slovenia is acknowledged. The authors are most grateful to Mr. Uwe Schachtely for his advice concerning the choice of nano- and microsilicas as well as Degussa AG for generous donation of silica samples.

REFERENCES

1. Karian, H. G., Ed. Handbook of Polypropylene and Polypropylene Composites; Marcel Dekker: New York, **2003**.
2. Wypych, G. Handbook of Fillers, 2nd ed.; ChemTec Publishing: Toronto, **2000**.
3. Rothon, R. N., Ed. Particulate-filled Polymer Composites, 2nd ed.; Rapra: Shawbury, **2006**.
4. Karger-Kocsis, J.; Fakirov, S., Eds. Preface. Nano- and Micromechanics of Polymer Blends and Composites; Carl Hanser Verlag: Munich, **2010**.
5. Rothon, R. N. In Functional Fillers for Plastics; Xanthos, M., Ed.; Wiley-VCH Verlag: Weinheim, **2010**.
6. Bikiaris, D. N.; Papageorgiou, G. Z.; Pavlidou, E.; Vouroutzis, N.; Palatzoglou, P.; Karayannidis, G. P. *J. Appl. Polym. Sci.* **2006**, *100*, 2684.
7. Rong, M. Z.; Zhang, M. Q.; Zheng, Y. X.; Zeng, H. M.; Walter, R.; Friedrich, K. *Polymer* **2001**, *42*, 167.
8. Wu, C. L.; Zhang, M. Q.; Rong, M. Z.; Friedrich, K. *Compos. Sci. Technol.* **2002**, *62*, 1327.
9. Zhou, T. H.; Ruan, W. H.; Mai, Y. L.; Rong, M. Z.; Zhang, M. Q. *Compos. Sci. Technol.* **2008**, *68*, 2858.
10. Pustak, A.; Leskovac, M.; Denac, M.; Švab, I.; Pohleven, J.; Makarovič, M; Musil, V.; Šmit, I. *J. Reinf. Plast. Compos.* **2014**, *33*, *851*.
11. Bracho, D; Dougnac, V. N.; Palza, H; Quijada, R. *J. Nano Mater.* **2012**, *2012*, 1.
12. Bikiaris, D. N.; Vassiliou, A.; Pavlidou, E.; Karayannidis, G. P. *Eur. Polym. J.* **2005**, *41*, 1965.
13. Buaziz, A.; Jaziri, M.; Dalmas, F.; Massardier, V. *Polym. Eng. Sci.* **2013**, *54*, 2187.
14. Chen, J. H.; Rong, M. Z.; Ruan, W. H.; Zhang, M. Q. *Compos. Sci. Technol.* **2009**, *69*, 252.
15. Uotila, R.; Hippi, U.; Paavola, S.; Seppala, J. *Polymer* **2005**, *46*, 7923.
16. Martin, G.; Barres, C.; Sonntag, P.; Garois, N.; Cassagnau, P. *Mater. Chem. Phys.* **2009**, *113*, 889.
17. Bazgir, S.; Katbab, A. A.; Nazockdast, H. *J. Appl. Polym. Sci.* **2004**, *92*, 2000.
18. Liu, Y.; Kontopoulou, M. *Polymer* **2006**, *47*, 7731.
19. Wang, W.-Z.; Liu, T. *J. Appl. Polym. Sci.* **2008**, *109*, 1654.
20. Mae, H.; Omiya, M.; Kishimoto, K. *J. Appl. Polym. Sci.* **2008**, *110*, 1145.
21. Panaitescu, D. M.; Vulunga, Z.; Notingher, P. V.; Nicolae, C. *Polym. Eng. Sci.* **2013**, *53*, 2081.

22. Panaitescu, D. M.; Vulunga, Z.; Radovici, C.; Nicolae, C. *Polym. Test.* **2012**, *31*, 355.
23. El-Midany, A. A.; Ibrahim, S. S. *Physicochem. Probl. Miner. Process.* **2011**, *46*, 295.
24. Long, Y.; Shanks, R. A. *J. Appl. Polym. Sci.* **1996**, *62*, 639.
25. Oksman, K.; Clemons, C. *J. Appl. Polym. Sci.* **1998**, *67*, 1503.
26. Stribeck, N.; Schneider, K.; Zeinolebadi, A; Li, X.; Sanporean, C.-G.; Vuluga, Z.; Iancu, S.; Duldner, M.; Santoro, G.; Roth, S. V. *Sci. Technol. Adv. Mater.* **2014**, *15*, 015004.
27. Pustak, A.; Denac, M.; Leskovac, M.; Švab, I.; Musil, V.; Šmit, I. Morphology and mechanical properties of iPP/silica composites modified with (styrene-b-ethylene-co-butylene-b-styrene) grafted with maleic anhydride, *submitted manuscript.*
28. Pustak, A.; Pucić, I.; Denac, M.; Švab, I.; Pohleven, J.; Musil, V.; Šmit, I. *J. Appl. Polym. Sci.* **2013**, *5*, 3099.
29. van Oss, C. J.; Giese, R. F.; Li, Z.; Murphy, K.; Norris, J.; Chaudhury, M. K.; Good, R. J. In Contact Angle, Wettability and Adhesion; Mittal, K. L., Ed.; VSP: Utrecht, **1993**; p 269.
30. Wu, S. *Polar J. Adhes.* **1973**, *5*, 39.
31. Urashita, S.; Kawakats, T.; Doi, M. *Progr. Theoret. Phys. Suppl.* **2000**, *138*, 412.
32. Premphet, K.; Horanont, P. *Polymer* **2000**, *41*, 9283.
33. Work, W. J.; Horie, K.; Hess, M.; Stepto, R. F. T. *IUPAC Pure Appl. Chem.* **2004**, *76*, 1985.
34. Steinmann, S.; Gronski, W.; Friedrich, C. *Polymer* **2002**, *43*, 4467.
35. Mittal, V., Ed. In Polymer Nanotube Nanocomposites: Synthesis, Properties, and Applications; Wiley: Hoboken, **2010**; Chapter 13.
36. Ma, C. G.; Mai, Y. L.; Rong, M. Z.; Ruan, W. H.; Zhang, M. Q. *Compos. Sci. Technol.* **2007**, *67*, 2997.
37. Reignier, J.; Favis, B. D.; Heuzey, M.-C. *Polymer* **2003**, *44*, 49.
38. Clarke, J.; Clarke, B.; Freakley, P. K.; Sutherland, I. *Plast. Rubber Compos.* **2001**, *30*, 39.
39. Sumita, M.; Sakata, K.; Asai, S.; Miyasaka, K.; Nakagawa, H. *Polym. Bull.* **1991**, *25*, 265.
40. Hobbs, S. Y.; Dekkers, M. E. J.; Watkins, V. H. *Polymer* **1988**, *29*, 1598.
41. Ray, S. S.; Bandyopadhyay, J.; Bousmina, M. *Eur. Polym. J.* **2008**, *44*, 3133.
42. Karger-Kocsis, J.; Kiss, L.; Kuleznev, V. N. *Polym. Commun.* **1984**, *44*, 122.
43. Hemmati, H. N.; Nazokdast, H.; Panahi, H. S. *J. Appl. Polym. Sci.* **2001**, *82*, 1129.
44. Das, S.; Murthy, V. S. R.; Murty, G. S. *J. Mater. Sci.* **1999**, *34*, 1347.
45. Fu, S.-Y.; Feng, X.-Q.; Lauke, B.; Mai, Y.-W. *Compos. B* **2008**, *39*, 933.
46. Gedde, U. W. Polymer Physics; Chapman and Hall: London, **1995**; Chapter 9.